Erosion of FEP Teflon and PMMA by VUV Radiation and Hyperthermal O or Ar Atoms

Jianming Zhang, Ned F. Lindholm, Amy L. Brunsvold, Hari P. Upadhyaya, and Timothy K. Minton*

Department of Chemistry and Biochemistry, Montana State University, Bozeman, Montana 59717

Masahito Tagawa

Department of Mechanical Engineering, Faculty of Engineering, Kobe University, Rokko-dai 1-1, Nada, Kobe 657-8501, Japan

ABSTRACT A combination of beam-surface-scattering, quartz-crystal-microbalance, and surface-recession experiments was conducted to study the effects of various combinations of O atoms [in the $O(^3P)$ ground state], Ar atoms, and vacuum ultraviolet (VUV) light on fluorinated ethylene−propylene copolymer (FEP) Teflon and poly(methyl methacrylate) (PMMA). A laser-breakdown source was used to create hyperthermal beams containing O and O_2 or Ar. A D_2 lamp provided a source of VUV light. O atoms with 4 eV of translational energy or less did not react with a pristine FEP Teflon surface. Volatile O-containing reaction products were observed when the O-atom energy was higher than 4.5 eV, and the signal increased with the O-atom energy. Significant erosion of FEP Teflon (~20% of Kapton H) was observed when it was exposed to the hyperthermal O/O_2 beam with an average O-atom energy of 5.4 eV. FEP Teflon and PMMA that were exposed to VUV light alone exhibited much less mass loss. Collision-induced dissociation by hyperthermal Ar atoms also caused mass loss, similar in magnitude to that caused by VUV light. There were no observed synergistic effects when VUV light or Ar bombardment was combined with O/O_2 exposure. For both FEP Teflon and PMMA, the erosion yields caused by simultaneous exposure to O/O_2 and either VUV light or Ar atoms could be approximately predicted by adding the erosion yield caused by O/O_2, acting individually, to the erosion yield caused by the individual action of either VUV light or Ar atoms.

KEYWORDS: FEP Teflon • PMMA • atomic oxygen • VUV light • collision-induced dissociation • polymer erosion • synergistic effects • low Earth orbit

1. INTRODUCTION

Spacecraft traveling in low Earth orbit (LEO) are subject to harsh environments, including ultraviolet (UV) and vacuum ultraviolet (VUV) radiation, thermal cycles, and high-energy collisions with atomic oxygen, molecular nitrogen, electrons, ions, and other charged particles (1−4). Fluorinated ethylene−propylene copolymer (FEP) Teflon, commonly used as a thermal control material on spacecraft, degrades upon exposure to the LEO environment (5−12). Many studies have used both space environments and ground-based test facilities in order to unravel the erosion mechanism of FEP Teflon. Some key factors that might be responsible for FEP Teflon erosion are atomic oxygen, VUV light, and collision-induced dissociation (CID) (13−21). Whether these factors act mainly alone or synergistically remains under debate.

It is well-known that FEP Teflon has strong absorption bands at VUV wavelengths (18, 22, 23). VUV radiation breaks C−C and C−F bonds and creates fragments that become volatile (18, 24). Skurat et al. (18) investigated the combined effect of VUV light and hyperthermal atomic oxygen on FEP Teflon and found that atomic oxygen had little effect on the mass loss of FEP Teflon. They further concluded that synergism between VUV light and fast atomic oxygen, if it exists, does not play any significant role. They also pointed out that, for fast atomic oxygen facilities that use electric discharges or laser-induced breakdown, intense VUV light can be produced along with atomic oxygen. Even though they did not exclude the reaction of oxygen with FEP Teflon, they suggested that the VUV light in the atomic oxygen source must be responsible to a great extent for the observed mass loss of FEP Teflon. It is worth noting, however, that the atomic oxygen beam used in Skurat et al.'s study had translational energies of 2−4 eV and that O atoms are not expected to react with pristine FEP Teflon at these energies (20). With the use of a synchronized chopper wheel to separate the VUV light from O atoms produced in an atomic oxygen source, Tagawa and co-workers (16, 17) studied the individual and combined effects of atomic oxygen and VUV light on the erosion of a fluorinated polymer deposited on a quartz-crystal microbalance (QCM). They found that 5-eV O atoms alone accounted for the majority of the erosion and that the effect of VUV light and O atoms together was an additive, not synergistic, effect. This result was consistent with an earlier investigation by Rutledge et al. in which they exposed FEP Teflon samples in various configurations to an oxygen plasma environment and determined that VUV light

* To whom correspondence should be addressed. Tel: 406-994-5394. Fax: 406-994-6011. E-mail: tminton@montana.edu.

Received for review November 20, 2008 and accepted January 15, 2009

DOI: 10.1021/am800186m

from the plasma had a negligible effect on the erosion yield (25). On the other hand, Koontz et al. suggested that there is a synergistic effect under the combined exposure of VUV light and atomic oxygen (13). However, this result was mainly based on thermal atomic oxygen. A synergistic effect was also found in a study of VUV and O^+ irradiation on FEP Teflon by Grossman et al. (14, 15), where the energy of O^+ was 50 eV.

The reactions of O atoms alone with fluorocarbon molecules have also been studied theoretically. With the use of the Hartree−Fock method and density functional theory, Gindulyte and co-workers (19) estimated a reaction barrier of 3−3.25 eV for reactions of $O(^3P)$ with fluoropolymer chains. They concluded that such reactions are possible under LEO conditions where the O atoms possess translational energy relative to a spacecraft on the order of 4.5 eV. Troya and Schatz (20) calculated the reactions of $O(^3P)$ with small fluorocarbons using quantum mechanical and molecular dynamics methods. They found that two reaction channels are possible, F elimination and direct C−C bond breakage, with the barriers of 3 and 2.5 eV, respectively. Direct C−C bond breakage was found to have a higher reaction cross section than F elimination. Compared to the reactions of $O(^3P)$ with the equivalent hydrocarbon molecules, both reaction channels have very low reaction probability even at a collision energy of 4.5 eV. However, the reaction cross sections increase rapidly as the collision energy increases above 4.5 eV.

In a series of beam-surface-scattering experiments, we have studied the individual and combined effects of VUV radiation and hyperthermal O/O_2 or Ar on FEP Teflon surfaces (24). We observed that O atoms alone do not react with pristine FEP Teflon even when they have translational energies up to 4 eV. Nevertheless, O-containing products appear and increase rapidly in flux when the O-atom energy increases above 4 eV. The signal also increases when there is an addition of VUV radiation. We also found that energetic collisions of O_2 or Ar may break chemical bonds and lead to the ejection of volatile products from an FEP Teflon surface. This CID process increased in probability with the translational energy of the bombarding species and was enhanced significantly in the presence of VUV radiation. Although several individual and combined effects were observed, the relative significance of these effects on the erosion of FEP Teflon remained unclear.

In this paper, we present a study of FEP Teflon erosion, which utilizes a combination of surface-recession and mass-loss measurements (with a profilometer and a quartz-crystal microbalance, respectively), with additional insight provided by beam-surface-scattering experiments. As a model VUV-light-sensitive polymer, poly(methyl methacrylate) (PMMA) was also included in this study. Atomic oxygen erodes PMMA, but relatively little is known about synergistic effects of hyperthermal atomic oxygen and VUV light on this material, and nothing is known about CID on PMMA surfaces. Individual and combined effects of O/O_2, Ar, and VUV light on the erosion of FEP Teflon and PMMA have been identified.

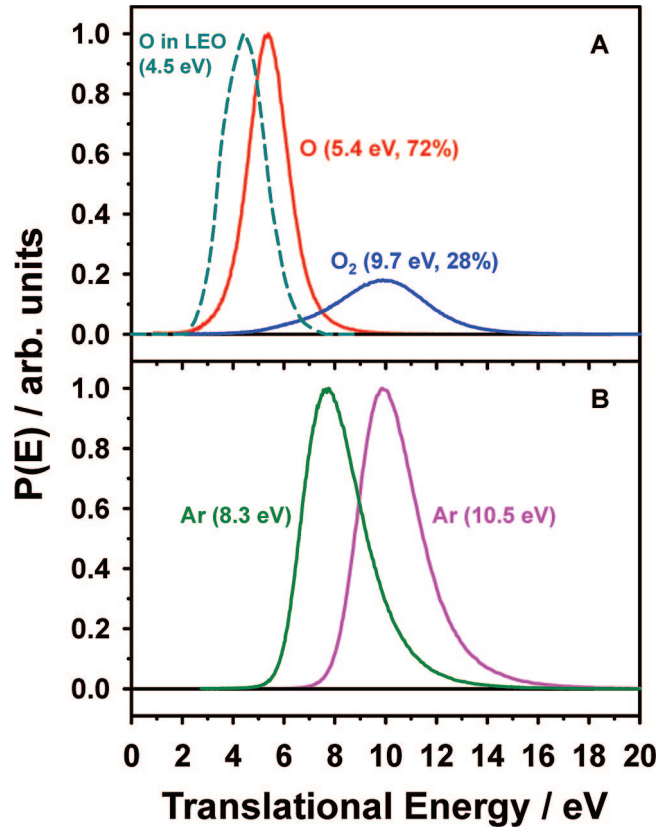

FIGURE 1. Translational energy distributions of hyperthermal O, O_2, and Ar beams used in our experiments. The average translational energies of each beam are shown. The translational energy distribution of atomic oxygen striking the ram surface of a spacecraft in LEO at an altitude of 400 km is plotted for comparison.

2. EXPERIMENTS

2.1. Exposures and Erosion-Depth Measurements. The exposure experiment was conducted in the source region of a molecular beam apparatus (26−30). Pulsed, hyperthermal beams containing O and O_2 (O/O_2) or Ar were produced by laser breakdown in a source that is similar to the original laser-breakdown source designed by Physical Sciences, Inc. (31). The O/O_2 beam contained 72% O and 28% O_2. The average translational energies of O and O_2 were 5.4 and 9.7 eV, respectively. The energy widths (full width at half-maximum, fwhm) for O and O_2 were 2 and 4 eV, respectively. Characterization of the beam has been performed to determine that the hyperthermal O atoms are in their ground electronic state, $O(^3P)$ (32), and that the O_2 molecules in the beam are in their $O_2(^3\Sigma_g^-)$ ground state (33). These results establish that the exposure environment used in our laboratory subjects materials to ground-state O and O_2. Hyperthermal Ar beams with average energies of 8.3 and 10.5 eV were used. The energy widths were 2.7 eV (fwhm). Translational energy distributions of the beams that were used in this experiment are shown in Figure 1. Figure 1 also shows the effective translational energy distribution of O atoms on ram surfaces in LEO at 400-km altitude (34). The average energy is ~4.5 eV, and the energy spread is about the same as that of the hyperthermal O atoms in our experiment. The laser-breakdown source also produces a broad spectrum of light, presumably from the IR to the VUV and possibly into the extreme ultraviolet (EUV). However, the spectrum and the intensity have not been measured.

Samples of test materials and of Kapton H (used for determination of the relative fluence) were exposed to the hyperthermal beams at a distance of 40 cm from the apex of the conical nozzle source. A detailed description of the sample mount can be found in an earlier paper (26). Nine samples can be exposed simultaneously. The FEP Teflon and Kapton H samples were punched from FEP Teflon and Kapton H sheets (American Durafilm Co. and Dupont, respectively), and each sample was 1.22 cm in diameter. PMMA samples were prepared by dropping a solution of 20 wt % PMMA (Scientific Polymer Products, Inc.; MW 15 000) in cholorobenzene on 1.22-cm-diameter germanium substrates and curing in a vacuum furnace (Centurion VPM) at 120 °C for 10 h. The PMMA thickness was typically >100 μm. A stainless-steel wire mesh was placed on top of each sample so that the erosion depth between the exposed and unexposed areas could be measured. The area of the hyperthermal beam was sufficient enough that all of the samples in the mount were exposed to an almost equal flux. All samples in these experiments where erosion depth was measured were exposed to 100 000 pulses of the hyperthermal beam. For this number of pulses, the Kapton-equivalent O-atom fluence was typically $\sim 2.3 \times 10^{20}$ O atoms cm^{-2}. After exposure, samples were removed from the chamber and examined by profilometry. The wire mesh allowed the measurement of many steps on the exposed samples with the use of a Dektak-3 (Veeco Metrology Group) surface profilometer. The average erosion depth and corresponding standard deviation for a given sample were calculated from measurements of 30−40 different step heights.

2.2. QCM Preparation. QCM samples were prepared on 0.5-in.-diameter QCM sensor disks. For PMMA samples, a solution of 20 wt % PMMA in chlorobenzene was spin-coated onto gold-coated QCM sensor disks at a spin rate of 2000 rpm for 60 s. After spin coating, the samples were allowed to dry in air and then placed in a vacuum furnace and cured at 120 °C for 10 h. The PMMA films on the QCM disks were determined by profilometry to be ~2 μm thick. For fluorocarbon samples, QCM disks were coated with fluorinated polymer films by a plasma-assisted physical vapor deposition technique developed at the Technology Research Institute of Osaka Prefecture (35). The thickness of the fluorinated polymer films was 156 nm. The morphology and chemical structure of the fluoropolymer films have not been characterized.

2.3. VUV Exposure. For VUV light irradiation, a 30-W D_2 lamp (Hamamatsu model L7292) was used. This lamp provided continuous VUV radiation mainly in the wavelength range of 115−200 nm. Such a D_2 lamp has been used extensively to simulate the effects of solar VUV light on materials in the LEO environment (36). The VUV exposure experiments were performed at two locations in the machine, one in the hyperthermal beam source chamber and one in the main scattering chamber. For VUV exposures in the source chamber, the samples were either QCM samples or mesh-covered samples, as described in section 2.1. The distance from the D_2 lamp to the samples was ~40 cm. At this distance, the samples experienced an irradiance of ~8 solar equivalents (or "suns") in the wavelength range 115−200 nm (37). In some experiments, a 1.5-in.-diameter LiF window was used to block the hyperthermal beam while still allowing the VUV light from the laser-breakdown source and/or from the D_2 lamp to reach the samples. Note that LiF has excellent transmission from the IR down to 104 nm (38, 39). With use of the LiF window, the effect of VUV light alone on the samples could be studied. When the VUV exposure experiments were performed in the main scattering chamber, the distance between the lamp and the samples was 15 cm. With the lamp at this distance, the sample surface experienced ~90 "suns" in the wavelength range 115−200 nm (37). The samples were irradiated with continuous VUV radiation, and time-of-flight (TOF) distributions of the products that

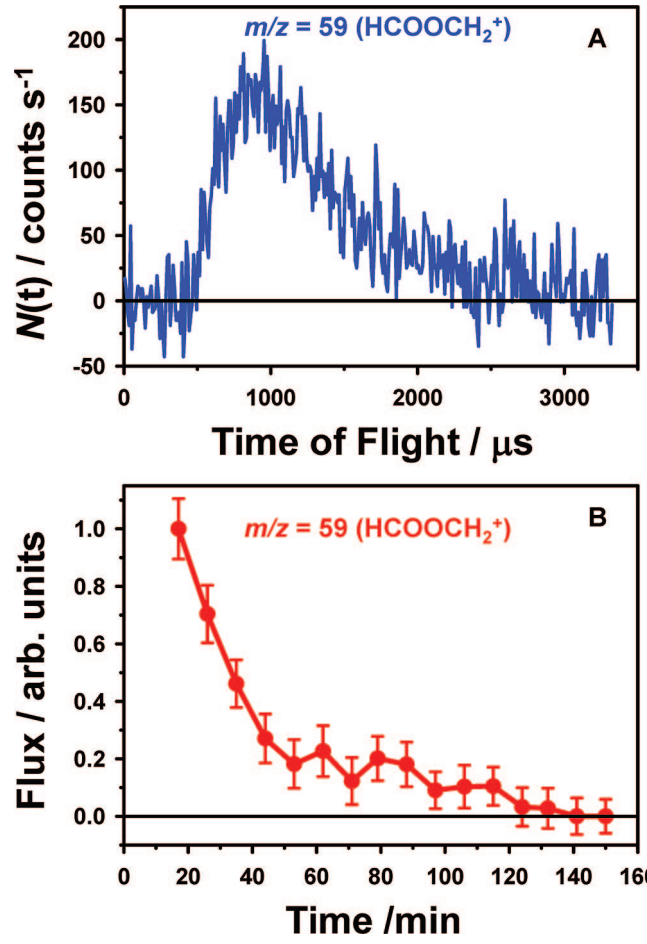

FIGURE 2. (A) Representative TOF distribution of volatile methyl formate ($HCOOCH_3$), detected at $m/z = 59$, emitted from a PMMA surface during exposure to an unfiltered D_2 lamp placed 15 cm from the surface. (B) Flux of methyl formate as a function of the exposure time.

emerged from the surface were detected with the mass spectrometer. A detailed description of the setup can be found in an earlier paper (24). TOF distributions at selected masses and detector angles were collected as a function of the arrival time at the detector ionizer, with modulation provided by a spinning slotted disk placed between the sample surface and the entrance of the detector, 29 cm from the ionizer.

2.4. Beam-Surface-Scattering Experiment. The beam-surface-scattering experiment was conducted in the main scattering chamber and has been described in detail previously (24). A major feature is the use of a synchronized chopper wheel between the source and sample surface. The chopper wheel not only blocks the VUV light from the hyperthermal beam source but also provides the ability to select narrowed portions of each overall beam. In the resulting translational energy distributions, the typical fwhm for O and O_2 are 1 and 2 eV, respectively. By variation of the synchronization of the chopper wheel with respect to the firing of the CO_2 laser, different portions (energy ranges) of the overall hyperthermal beam pulse may be selected, thus allowing an investigation of the translational energy dependence on reactivity.

3. RESULTS AND DISCUSSION

Photodegradation of PMMA is initiated with the removal of the ester group and the formation of volatile methyl formate, $HCOOCH_3$, which leads to mass loss (40−43). Figure 2A shows a representative TOF distribution of methyl

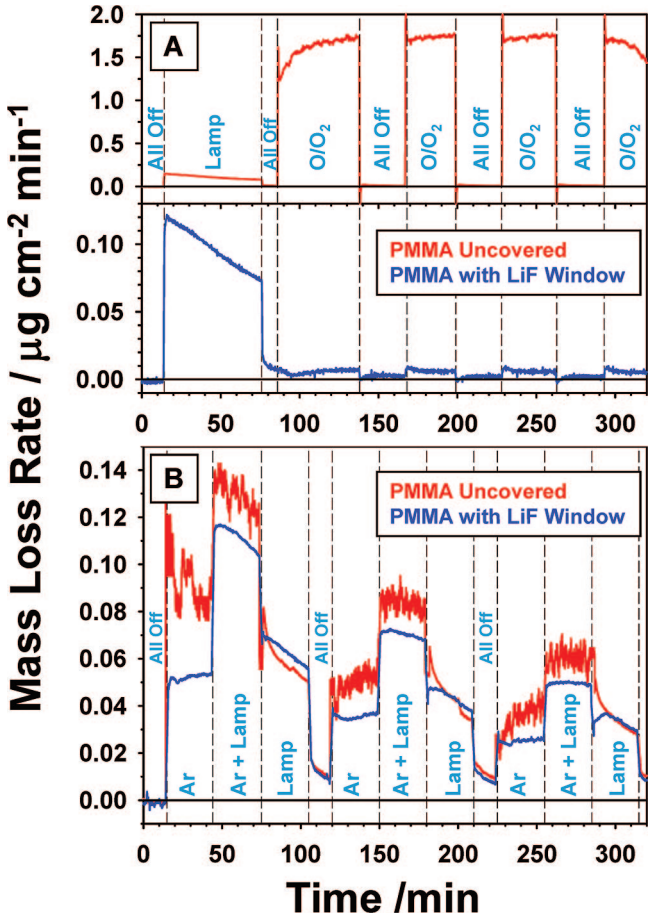

FIGURE 3. PMMA mass-loss rate as a function of the exposure time for (A) O/O_2 beam exposure and (B) Ar beam exposure. The red curves correspond to uncovered samples. The blue curves correspond to samples covered by a LiF window. Different exposure conditions were chosen during different time periods, as indicated. "Lamp" means that the samples were only exposed to the D_2 lamp. "O/O_2" or "Ar" means that the samples were only exposed O/O_2 or Ar beams, respectively. "Ar + Lamp" means that the samples were exposed simultaneously to both the Ar beam and the D_2 lamp.

formate, detected at a mass-to-charge ratio, *m*/*z*, of 59 ($HCOOCH_2^+$), which was emitted from a PMMA surface upon exposure to the D_2 lamp in the main scattering chamber. The flux of emitted methyl formate decreases with time, as shown in Figure 2B. This decrease is relatively rapid, presumably because the VUV flux on the surface is high (~90 suns in LEO). The removal of the ester group also leads to the formation of C−C double bonds and cross-linking. The rate of methyl formate liberation from a PMMA film has been described by a diffusion model and has also been linked with the thinning of the film (40).

The mass-loss rate for PMMA samples, determined from QCM measurements, is shown in Figure 3. The QCM allowed the mass loss of two samples, placed side-by-side, to be measured simultaneously. For each exposure, a LiF window covered one sample in order to block O/O_2 or Ar in the hyperthermal neutral beam while allowing VUV light in the beam to reach the samples. Therefore, the amount of erosion caused by the VUV light in the hyperthermal beams could be evaluated. In the figure, the notation "Lamp" means that the samples were exposed only to the D_2 lamp. "O/O_2" or "Ar" means that the samples were exposed only to the hyperthermal O/O_2 or Ar beams. "Ar + Lamp" means that the samples were exposed simultaneously to both the Ar beam and the D_2 lamp. As shown in the first trace in the bottom panel of Figure 3A, PMMA erodes significantly from the D_2 lamp radiation, and the mass-loss rate decreases with the exposure time. Subsequent traces in the bottom panel of Figure 3A, which show the mass loss of the covered sample when the O/O_2 beam is on, reveal that the mass-loss rate caused by the VUV light from the O/O_2 source is insignificant, only ~10% of that caused by the D_2 lamp and ~0.5% of that caused by the O/O_2 beam on the uncovered sample (upper panel in Figure 3A). Given that the approximate VUV flux of the D_2 lamp is ~8 suns in LEO, the mass loss of the covered PMMA sample suggests that the effective VUV flux from the O/O_2 source is slightly less than 1 sun. On the other hand, when PMMA is exposed to the hyperthermal Ar beam, as shown in the first section of Figure 3B, the mass-loss rate caused by the VUV light in the Ar beam is comparable to that caused by the D_2 lamp. It appears that the effective VUV light intensity in the Ar beam is at least 5 times higher than that in the O/O_2 beam. When the traces in Figure 3B that give the mass-loss rate for the Ar beam with and without the LiF window are compared, it is clear that collisions of Ar atoms also contribute significantly to the mass loss, presumably through CID. This conclusion is reached by assuming that the EUV light from the source with wavelengths below the LiF cutoff of 104 nm has a negligible effect on the mass loss compared to the effect of the VUV light that is transmitted by the LiF window. The mass-loss rate caused by CID, as indicated by the difference between the traces for covered and uncovered samples during Ar exposure, decreases with time. The mass-loss rate caused by the D_2 lamp exposure also decreases with time. Presumably, the decrease in the mass-loss rate caused by either CID or photodissociation decreases with time in part because photoinduced and collision-induced degradation of PMMA lead to cross-linking near the surface and concomitant reduction in the ease by which volatile products can be liberated. In addition, the mass-loss rate is expected to decrease as the available methyl formate products are used up. When adjacent traces for "Ar", "Ar + Lamp", and "Lamp" are compared, it can be concluded that the mass-loss rate resulting from the combination of the D_2 lamp and the Ar beam is slightly less than the sum of the mass-loss rates resulting from the D_2 lamp and the Ar beam acting individually. Perhaps the combination of VUV light from the Ar beam source and the lamp removes volatile products at a high enough rate that Ar atoms find fewer pathways by which to eject volatile products (by CID) than they do when the radiation from the lamp is not present. Because Ar collisions are always accompanied by VUV (and/or EUV) light from the beam source, a determination of whether or not there is a minor synergistic effect between VUV light and Ar collisions cannot be drawn from this measurement.

QCM measurements of mass-loss rates for fluorinated polymer films, under a variety of exposure conditions, are

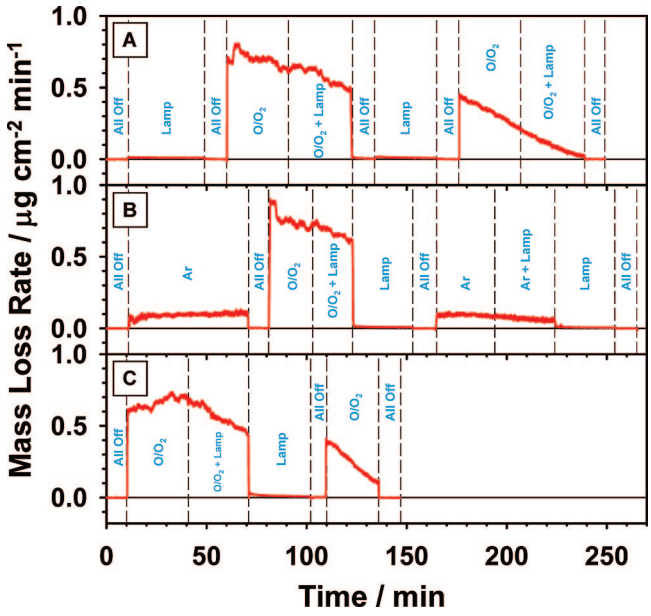

FIGURE 4. Mass-loss rates of three different samples (A–C) of a fluorocarbon polymer film as a function of the exposure time under different exposure conditions as shown. The samples were not covered by a LiF window. Different exposure sequences and conditions were chosen for each sample, as indicated.

presented in Figure 4. The samples were not covered with a LiF window during the exposures. In the exposure sequence shown in Figure 4A, the sample was first exposed to the D_2 lamp, followed by exposure to the O/O_2 beam, and then simultaneous exposure of the O/O_2 beam and the D_2 lamp. The mass-loss rate caused by VUV light from the D_2 lamp is less than 2% of that caused by the O/O_2 beam. During O/O_2 exposure, the mass-loss rate decreases with time, even when the VUV light is added to the exposure. Apparently, the fluorinated polymer film on the QCM disk was so thin that the mass-loss rate caused by O/O_2 continued to decrease until the film was eroded through. In the first exposure sequence (Figure 4A), the sample was completely eroded at 240 min. In the exposure sequence shown in Figure 4B, the sample was exposed first to the Ar beam, followed by O/O_2 exposure, and then the D_2 lamp (with and without O/O_2). The mass-loss rate caused by the Ar beam was about 14% of that caused by the O/O_2 beam. On the basis of the results presented in Figure 3B, the erosion caused by VUV (and/or EUV) light in the Ar beam is about equal to that caused by the D_2 lamp. Given the extremely small mass-loss rate caused by the D_2 lamp alone and assuming a similar effect of the VUV light from the D_2 lamp and from the Ar beam source, the majority (~90%) of the erosion of the fluoropolymer film must have been caused by CID from Ar. In the exposure sequence shown in Figure 4C, the sample was first exposed to the O/O_2 beam, followed by additional D_2 lamp exposure. The initial erosion rate caused by O/O_2 (in the first 10 min) is slightly less than that with pre-exposure by the D_2 lamp or the Ar beam. After the first 10 min of exposure and before the film starts to erode through, the mass-loss rates are similar. The difference in the initial erosion rate is consistent with a mechanism in which pre-exposure by VUV light or Ar atoms can create radical sites on the surface, through photodissociation or CID, and enhance the initial reactivity with the O/O_2 beam. Once the reactivity with O and/or O_2 in the beam reaches a steady state, the contributions from VUV light or Ar atoms are not significant compared to the reactivity with the O/O_2 beam. It thus appears that the pre-exposure by VUV light or Ar atoms may speed the approach to steady-state O (and, perhaps, O_2) reactions but that the VUV light or Ar atoms cause negligible mass loss compared to the O/O_2 beam.

A summary of the erosion-depth measurements from various exposures is presented in Table 1. Except for Kapton H reference samples, the numbers reported in the table come from averages of recession measurements for two or three identical samples that were exposed at different positions on the sample mount. An exposure with the D_2 lamp alone was conducted for 55.5 h in order to obtain significant enough erosion that it could be measured with reasonable precision. The table also lists the equivalent 14-h measurement. (Note that 14 h was the exposure duration for 100 000 pulses of the hyperthermal beam.) For PMMA samples, the equivalent 14-h measurement is based on the time dependence of PMMA mass loss under irradiation from the D_2 lamp, as measured by the QCM and fitted with a function. For FEP Teflon samples, the equivalent 14-h measurement is based on the assumption that the material erodes linearly with time. The PMMA erosion from the D_2 lamp alone is comparable to that from the VUV (and/or EUV) light from the source that produces a 10-eV Ar beam, which is consistent with our QCM measurement shown in Figure 3B. The erosion depth for uncovered PMMA samples in the 10-eV Ar beam is ~60% higher than that for covered PMMA samples, which must be the result of CID by Ar, assuming negligible erosion from any EUV radiation that might be produced by the Ar source. The erosion depth for uncovered PMMA samples in the 10-eV Ar beam is slightly higher than that in the 8-eV Ar beam. This slight increase in the erosion depth is probably related to the difference in Ar collision energy, assuming that the intensities of VUV (and/or EUV) light in the two Ar beams are similar. A comparison of the PMMA erosion for 8-eV Ar beams with and without the D_2 lamp indicates an effect that is less than additive, which is probably because the PMMA mass-loss rate caused by VUV light is limited by diffusion of methyl formate out of the film (40). When the covered PMMA samples were exposed to the O/O_2 beam, they were only slightly eroded. The erosion pattern was visible, but the erosion depth was under the detection limit of our profilometer, which is ~0.1 μm on these relatively rough surfaces. The erosion of PMMA by VUV light, from either the D_2 lamp or the VUV light in the O/O_2 beam, is negligible compared to the erosion of the uncovered PMMA sample in the O/O_2 exposure. Given the uncertainties in the erosion-depth measurements, the erosion depths of PMMA caused by the O/O_2 beam alone and in combination with the D_2 lamp are roughly the same, again reflecting the negligible effect of the VUV light in comparison with O/O_2.

The erosion results for the FEP Teflon samples are analogous to those for the PMMA samples. The LiF-covered

Table 1. Erosion-Depth Measurements of Exposed FEP Teflon and PMMA Samples[a]

exposure condition	uncovered FEP Teflon (μm)	uncovered PMMA (μm)	FEP Teflon covered with LiF window (μm)	PMMA covered with LiF window (μm)	Kapton H (μm)
55.5-h D_2 lamp	0.35 ± 0.05	0.41 ± 0.07	–	–	no erosion
equivalent 14-h D_2 lamp	0.09 ± 0.01[b]	0.25 ± 0.04[c]	–	–	no erosion
14-h O/O_2	1.22 ± 0.14	10.9 ± 1.1	no erosion	<0.1	7.0 ± 0.1
14-h $O/O_2 + D_2$ lamp	1.46 ± 0.12	10.4 ± 1.1	–	–	7.1 ± 0.1
14-h Ar (8 eV)	0.12 ± 0.03	0.32 ± 0.05	–	–	no erosion
14-h Ar (8 eV) + D_2 lamp	0.24 ± 0.03	0.42 ± 0.06	–	–	no erosion
14-h Ar (10 eV)	0.15 ± 0.02	0.39 ± 0.05	no erosion	0.24 ± 0.04	

[a] The errors represent the standard deviation ($\pm\sigma$) of 30–40 measurements taken on 1–3 samples of each type. The dash symbol, " – ", means there was no sample exposed under that condition. "No erosion" means there is no erosion pattern on the sample visible with the naked eye or optical microscope. "< 0.1" means there is a visible erosion pattern, but the erosion depth is too small to be accurately determined with our profilometer. [b] Converted from "55.5-h D_2 lamp" based on a linear relationship. [c] Converted from "55.5-h D_2 lamp" based on our QCM measurement of mass loss as a function of the exposure time.

FEP Tefon samples have no observable erosion pattern, which indicates that the VUV light in both the Ar and O/O_2 beams may only negligibly erode FEP Teflon. The small erosion depths caused by exposure of FEP Teflon to the 8- and 10-eV Ar beams suggest that hyperthermal Ar atoms may erode this material by CID. There is also a small enhancement in the erosion when the Ar beam energy increases from 8 to 10 eV. In our previous beam-surface-scattering experiment (24), we found that the flux of CID products increases exponentially with beam energy once it rises above 8 eV. Both our surface-recession and beam-surface-scattering results are consistent with theoretical calculations by Troya and co-workers (44, 45). Their studies on $Ar + CF_4$ and $Ar + C_2F_6$ collisions suggest that CID of the perfluorocarbon molecule may be more likely than its hydrocarbon analogue, CH_4 or C_2H_6. Thus, for collisions of a given energy, CF_4 or C_2F_6 is more susceptible to CID than CH_4 or C_2H_6. The FEP Teflon erosion depth for the 8-eV Ar beam with the D_2 lamp is 0.24 μm, which is similar to the sum of the erosion depths caused by exposure to the D_2 lamp and the 8-eV Ar beam. This observation indicates an additive effect between the Ar beam and the D_2 lamp. Our previous beam-surface-scattering experiment (24) showed that the flux of the CID products was enhanced in the presence of VUV light. As discussed in connection with the results of the QCM experiments on PMMA, our erosion-depth measurements cannot exclude the VUV (and/or EUV) light from the Ar beam source. The additive effect observed here appears to correspond simply to an addition of VUV light from the D_2 lamp. Nevertheless, the erosion caused by pure CID or synergism between CID and VUV light is not significant. On the other hand, the O/O_2 beam erodes FEP Teflon significantly. The erosion depth for FEP Teflon is about 17% of that for Kapton H. Considering the densities of FEP Teflon (2.14 g/cm^3) and Kapton H (1.42 g/cm^3), the mass loss of FEP Teflon is about one-third of that of Kapton H. Given the facts that the LiF-covered FEP Teflon sample in the O/O_2 beam hardly eroded and that the QCM measurements with the fluoropolymer (Figure 4) indicated no synergistic effect, it is highly doubtful that the VUV component in the O/O_2 beam contributes to the observed erosion depth of FEP Teflon. The O_2 component in the O/O_2 beam has sufficient energy (average energy ~10 eV) to cause CID of FEP Teflon. However, this CID effect on FEP Teflon erosion would be insignificant. The O_2 intensity in the O/O_2 beam is less than 25% of the intensity of Ar atoms in the Ar beams, and the effective flux of VUV (and/or EUV) light in the O/O_2 beam is less than 20% of that in the Ar beams, based on a comparison of PMMA mass loss. As seen in Table 1, the erosion depth of uncovered FEP Teflon for the 10-eV Ar exposure is 0.15 μm, the majority of which is caused by CID. Twenty-five percent of this surface recession is 0.038 μm, which is about 3% of the erosion depth observed for O/O_2 exposure. Therefore, the contribution of the CID and VUV (and/or EUV) light to the erosion of FEP Teflon by the O/O_2 beam is probably less than 3%. There is a small enhancement in the erosion with the addition of the D_2 lamp, which appears to be roughly an additive effect. This result is consistent with the work by Tagawa and co-workers (16, 17), who used a synchronized chopper wheel to block the VUV (and/or EUV) light from their atomic-oxygen source, found that 5-eV O atoms alone account for the majority of the erosion of their fluorinated polymer, and concluded that the effect of VUV and O atoms together was an additive, not synergistic, effect.

The results on FEP Teflon erosion, in combination with the PMMA results, lead us to the conclusion that O atoms, and perhaps O_2 molecules, in our hyperthermal O/O_2 beam react with FEP Teflon directly. This conclusion is strongly supported by our beam-surface scattering experiment, as well as experimental and theoretical results from other groups. Figure 5 shows TOF distributions of an O-containing product, detected at a mass-to-charge ratio of $m/z = 47$ (CFO^+), at different O-atom energies. It is important to point out that the O/O_2 beams used for the beam-surface scattering experiment utilized a synchronized chopper wheel so that the VUV (and/or EUV) light in the beam was blocked. The figure shows that the CFO^+ signal (with a flight time in the vicinity of 200 μs) appears at an O-atom energy of ~4.4 eV and increases with beam energy. We have observed similar behavior for another O-containing product, detected at $m/z = 66$ (CF_2O^+). Note that CFO^+ and CF_2O^+ signals were also observed in an earlier study that reported the mass spectra of volatile products formed when a hyperthermal O-atom beam bombarded an FEP Teflon surface (21). We should also point out that the signals for CFO^+ and CF_2O^+ are very weak. Nevertheless, the observation of O-containing signals in the absence of any VUV radiation is direct evidence of O-atom reactions with pristine FEP Teflon. Once there are radical sites at the FEP Teflon surface, the O_2 molecules in the beam may also react with it. This is supported by an

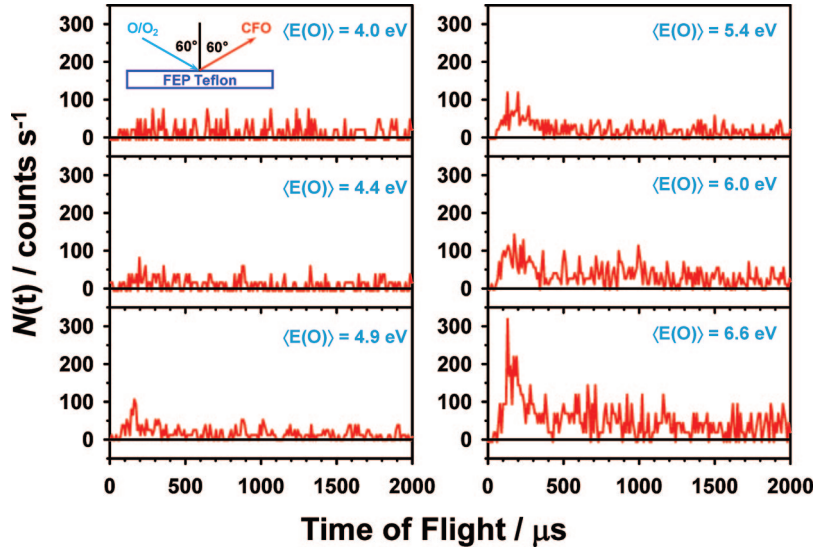

FIGURE 5. Representative TOF distributions of reactively scattered, O-containing products, detected at $m/z = 47$ (CFO^+), following the bombardment of a pristine FEP Teflon surface by hyperthermal O/O_2 beams at different translational energies. The incidence and detection angles were both 60° with respect to the surface normal. The incidence energy in each panel is the average translational energy of the O atoms in the beam; the incidence energy of O_2 is twice as high.

electron spin resonance study by Rasoul et al. (23), who observed peroxy radicals on a VUV-exposed FEP Teflon surface when it was exposed to air. As mentioned in the Introduction, Gindulyte and co-workers calculated a reaction barrier of 3−3.25 eV for reactions of $O(^3P)$ with fluoropolymer chains. They thus concluded that such reactions are possible at a collision energy of 4.5 eV. Troya and Schatz (20) performed calculations on the reactions of $O(^3P)$ with small fluorocarbons and found two reaction channels, F elimination and direct C−C bond breakage, with barriers of 3 and 2.5 eV, respectively. Direct C−C bond breakage has a higher reaction cross section, but both reaction cross sections are very low even at a collision energy of 4.5 eV. Above that, the reaction cross sections increase rapidly with the collision energy, which is consistent with what is observed in the data shown in Figure 5.

The experiments described above give us the origin of FEP Teflon erosion in the exposure environment created by the laser-breakdown O/O_2 source in our apparatus. Even though the mechanisms of FEP Teflon erosion depend on the details of the exposure environment, the insight gained here may still help explain the erosion of FEP Teflon in LEO and in other ground-based test environments that contain atomic oxygen. In the LEO environment, for example, at 400 km altitude, the average O-atom impact energy is about 4.5 eV with a fwhm of 2 eV, as shown in Figure 1A. At these collision energies, especially in the higher-energy part of the distribution, O atoms can react directly with FEP Teflon and produce volatile $C_mF_nO_p$ (where m, n, and p are integers greater than or equal to zero) products and carry mass away from the surface. Collisions of charged particles and ions may also contribute to FEP Teflon erosion. Note that the intensity of the VUV light from the lamp in our exposure experiment is about 8 "suns" and the O-atom flux is similar to or larger than that in LEO. Moreover, both the flux and energy of Ar atoms in our exposure experiment are much higher than those of N_2 molecules in LEO. Yet in our QCM and erosion-depth experiments, the effects of VUV light and CID on the erosion of the fluorinated polymer film and FEP Teflon are small. Therefore, the solar VUV and CID from N_2 collisions in the LEO environment are not expected to contribute significantly to FEP Teflon erosion. The VUV light and CID can produce radical sites on an FEP Teflon surface and enhance O-atom reactivity, as discussed in connection with Figure 4. Nevertheless, we have seen much evidence that hyperthermal O atoms can react directly with an FEP Teflon surface, and such direct reactions likely dominate the erosion of the surface at moderate fluxes of VUV photons or energetic collisions. As a final note, the FEP Teflon erosion yield measured in our laboratory, i.e., 5.2×10^{-25} cm^3 per O atom, is about 17% that of Kapton H, although the erosion yield of FEP Teflon in LEO is typically much lower, 6.7% that of Kapton H from an experiment on the International Space Station (46). The higher relative erosion yield of FEP Teflon that we observe is likely the result of the relatively high O-atom energies used in the laboratory experiments. The average effective energy of an O atom striking a surface on orbit is ~4.5 eV, whereas our experiments utilized an average O-atom energy of 5.4 eV. This difference is not so significant for Kapton H, which erodes readily under attack from O atoms with either energy. However, the reactivity of FEP Teflon with O atoms increases dramatically as the O-atom energy rises from 4.5 to 5.4 eV, making the difference between the effective O-atom collision energy in space and the O-atom energy in our laboratory significant.

4. CONCLUSION

Mass-loss and erosion-depth measurements, as well as beam-surface scattering experiments, have been conducted to probe the individual and combined effects of VUV light, high-energy collisions, and atomic oxygen on the erosion of FEP Teflon and PMMA. The results for FEP Teflon and PMMA are similar: (1) VUV light breaks bonds and leads to volatile products and mass loss. (2) Energetic collisions of Ar with

>8 eV translational energy also break bonds through CID and lead to volatile products and mass loss. (3) O atoms with translational energies of less than ~4.4 eV do not react with pristine FEP Teflon. Once above this energy, O atoms can react directly with FEP Teflon, and the reactivity increases rapidly with the O-atom energy. (4) The erosion yields of FEP Teflon and PMMA by the hyperthermal O/O_2 beam in our apparatus are significant, ~17% and ~150% of Kapton H, respectively. (5) The contributions of VUV light and CID to the erosion of FEP Teflon and PMMA are not significant compared to that of O/O_2 exposure. (6) There is no synergistic effect between O atoms and VUV light or CID in the erosion of FEP Teflon or PMMA.

Acknowledgment. This work was supported by grants from the Air Force Office of Scientific Research (Grants FA9550-04-1-0428 and FA9550-07-C-0139).

REFERENCES AND NOTES

(1) Champion, K. S. W.; Cole, A. E.; Kantor, A. J. Standard and Reference Atmospheres In *Handbook of Geophysics and the Space Environment*; Jursa, A. S., Ed.; Air Force Geophysics Laboratory, United States Air Force: Hanscom, AFB, 1985; Chapter 14.

(2) Minton, T. K.; Garton, D. J. Dynamics of Atomic-Oxygen-Induced Polymer Degradation in Low Earth Orbit. In *Advanced Series in Physical Chemistry, Vol. 11, Chemical Dynamics in Extreme Environments*; Dressler, R. A., Ed.; World Scientific: Singapore, 2001; pp 420–489.

(3) Murad, E. *J. Spacecr. Rockets* **1996**, *33*, 131.

(4) Roble, R. G. Energetics of the Mesosphere and Thermosphere In *The Upper Mesosphere and Lower Thermosphere: A Review of Experiment and Theory*; Johnson, R. M., Killeen, T. L., Eds.; American Geophysical Union: Washington, DC, 1995; pp 1–21.

(5) Banks, B. A. The Use of Fluoropolymers in Space Applications In *Modern Fluoropolymers*; Schiers, J., Ed.; John Wiley: Chichester, U.K., 1997; pp 103–113.

(6) de Groh, K. K.; Gaier, J. R.; Hall, R. L.; Espe, M. P.; Cato, D. R.; Sutter, J. K.; Scheiman, D. A. *High Perform. Polym.* **2000**, *12*, 83.

(7) de Groh K. K., Smith, D. C. Investigation of Teflon FEP Embrittlement on Spacecraft in Low Earth Orbit. *The 7th International Symposium on Materials in a Space Environment*, Toulouse, France, June 16–20,1997; Guyenne, T. D., Ed.; European Space Agency: Paris, France, 1997; pp 255–265; ESA SP-399.

(8) Dever, J. A.; de Groh, K. K.; Banks, B. A.; Townsend, J. A. *High Perform. Polym.* **1999**, *11*, 123.

(9) Dever, J. A.; de Groh, K. K.; Banks, B. A.; Townsend, J. A.; Barth, J. L.; Thomson, S.; Gregory, T.; Savage, W. *High Perform. Polym.* **2000**, *12*, 125.

(10) Dever, J. A.; de Groh, K. K.; Messer, R. K.; McClendon, M. W.; Viens, M.; Wang, L. L.; Gummow, J. D. *High Perform. Polym.* **2001**, *13*, S373.

(11) Stiegman, A. E.; Brinza, D. E.; Laue, E. G.; Anderson, M. S.; Liang, R. H. *J. Spacecr. Rockets* **1992**, *29*, 150.

(12) Townsend, J. A.; Hansen, P. A.; McClendon, M. W.; de Groh, K. K.; Banks, B. A. *High Perform. Polym.* **1999**, *11*, 63.

(13) Koontz, S.; Leger, L.; Albyn, K.; Cross, J. *J. Spacecr. Rockets* **1990**, *27*, 346.

(14) Grossman, E.; Noter, Y.; Lifshitz, Y. Oxygen and VUV Irradiation of Polymers: Degradation Mechanism and Synergistic Processes. *7th International Symposium on Materials in a Space Environment*, Toulouse, France, June 16–20, 1997; Guyenne, T. D., Ed.; European Space Agency: Paris, France, 1997; pp 217–223; ESA SP-399.

(15) Grossman, E.; Gouzman, I. *Nucl. Methods Methods Phys. Res. B* **2003**, *208*, 48.

(16) Tagawa, M.; Abe, S.; Kishida, K.; Yokota, K.; Okamoto, A. Effect of EUV from the Oxygen Plasma in the Ground-Based Atomic Oxygen Test of Fluorinated Polymer. *Proceedings of the 26th International Symposium on Space Technology and Sciences*, Hamamatsu, Japan, 2008, on CD-ROM.

(17) Tagawa, M.; Abe, S.; Kishida, K.; Yokota, K.; Okamoto, A. Synergistic Effect of EUV from the Laser-Sustained Oxygen Plasma in the Ground-Based Atomic Oxygen Simulation of Fluorinated Polymers. *Proceedings of the 9th International Conference on the Protection of Materials and Structures in a Space Environment*, Toronto, Canada, May 20–23, 2008.

(18) Skurat, V. E.; Samsanov, P. V.; Nikiforov, A. P. *High Perform. Polym.* **2004**, *16*, 339.

(19) Gindulyte, A.; Massa, L.; Banks, B. A.; Miller, S. K. R. *J. Phys. Chem. A* **2002**, *106*, 5463.

(20) Troya, D.; Schatz, G. C. Theoretical Study of Reactions of Hyperthermal $O(^3P)$ with Perfluorinated Hydrocarbons. *Proceedings of the 7th International Conference on the Protection of Materials and Structures in a Space Environment*, Toronto, Canada, May 10–13, 2004.

(21) Cazaubon, B.; Paillous, A.; Siffre, J. *J. Spacecr. Rockets* **1998**, *35*, 797.

(22) Seki, K.; Tanaka, H.; Ohta, T.; Aoki, Y.; Imamura, A.; Fujimoto, H.; Yamamoto, H.; Inokuchi, H. *Phys. Scr.* **1990**, *41*, 167.

(23) Rasoul, F. A.; Hill, D. J. T.; George, G. A.; O'Donnell, J. H. *Polym. Adv. Technol.* **1998**, *9*, 24.

(24) Brunsvold, A. L.; Upadhyaya, H. P.; Zhang, J.; Minton, T. K. *ACS Appl. Mater. Interfaces* **2009**, *1*, 1.

(25) Rutledge, S. K.; Banks, B. A.; Kitral, M. A Comparison of Space- and Ground-Based Facility Environmental Effects for FEP Teflon. In *Space Technology Proceedings, Vol. 4, Protection of Space Materials from the Space Environment*; Kleiman, J. I., Tennyson, R. C., Eds.; Kluwer: Dordrecht, The Netherlands, 2001; pp 165–179.

(26) Buczala, D. M.; Brunsvold, A. L.; Minton, T. K. *J. Spacecr. Rockets* **2006**, *43*, 421.

(27) Brunsvold, A. L.; Minton, T. K.; Gouzman, I.; Grossman, E.; Gonzalez, R. *High Perform. Polym.* **2004**, *16*, 303.

(28) Cooper, R.; Upadhyaya, H. P.; Minton, T. K.; Berman, M. R.; Du, X.; George, S. M. *Thin Solid Films* **2007**, *516*, 4036.

(29) Zhang, J.; Garton, D. J.; Minton, T. K. *J. Chem. Phys.* **2002**, *117*, 6239.

(30) Zhang, J.; Upadhyaya, H. P.; Brunsvold, A. L.; Minton, T. K. *J. Phys. Chem. B* **2006**, *110*, 12500.

(31) Caledonia, G. E.; Krech, R. H.; Green, D. B. *AIAA J.* **1987**, *25*, 59.

(32) Garton, D. J.; Minton, T. K.; Maiti, B.; Troya, D.; Schatz, G. C. *J. Chem. Phys.* **2003**, *118*, 1585.

(33) Troya, D.; Schatz, G. C.; Garton, D. J.; Brunsvold, A. L.; Minton, T. K. *J. Chem. Phys.* **2004**, *120*, 731. This study led to the conclusion that any O_2 in the hyperthermal O/O_2 beam must be in the ground $^3\Sigma_g^-$ state, because the experiment was not able to identify an H_2O product that was predicted by theory to be indicative of an $O_2(^1\Delta)$ reaction: $O_2(^1\Delta) + CH_4 \rightarrow H_2O + H_2CO$.

(34) Banks, B. A.; de Groh, K. K.; Rutledge, S. K.; DiFilippo, F. J. *NASA/TM* **1996**, 107209.

(35) Okamoto, A.; Matsunaga, S. The modification of fluorocarbon resin composite thin film by plasma assist film formation method. *Book of Abstracts, the 45th Annual Symposium of the Vacuum Society of Japan (ASVSJ-45)*; 2004; p 72 (in Japanese).

(36) Dever, J. A.; Pietromica, A. J.; Stueber, T. J.; Sechkar, E. A.; Messer, R. K. *NASA/TM* **2002**, 211337.

(37) Dever J. A. Personal Communication.

(38) Laufer, D. H.; Pirog, J. A.; McNesby, J. R. *J. Opt. Soc. Am.* **1965**, *55*, 64.

(39) Heath, P.; Sacher, P. *Appl. Opt.* **1966**, *15*, 937.

(40) Cisse, A. L.; Grossman, E.; Sibener, S. J. *J. Phys. Chem. C* **2008**, *112*, 7167.

(41) Choi, J. O.; Moore, J. A.; Corelli, J. C.; Silverman, J. P.; Bakhru, H. *J. Vac. Sci. Technol. B* **1988**, *6*, 2286.

(42) Okudaira, K. K.; Hasegawa, S.; Sprunger, P. T.; Morikawa, E.; Saile, V.; Seki, K.; Harada, Y.; Ueno, N. *J. Appl. Phys.* **1998**, *83*, 4292.

(43) Okudaira, K. K.; Morikawa, E.; Hasegawa, S.; Sprunger, P. T.; Saile, V.; Seki, K.; Harada, Y.; Ueno, N. *J. Electron Spectrosc. Relat. Phenom.* **1998**, *88–91*, 913.

(44) Troya, D. *J. Phys. Chem. A* **2005**, *109*, 5814.

(45) Tasic, U.; Hein, P.; Troya, D. *J. Phys. Chem. A* **2007**, *111*, 3618.

(46) de Groh, K.; Banks, B. A.; McCarthy, C. E.; Rucker, R. N.; Roberts, L. M.; Berger, L. A. *High Perform. Polym.* **2008**, *20*, 388.

AM800186M